Laser-induced plasmas in ambient air for incoherent broadband cavity-enhanced absorption spectroscopy

Albert A. Ruth[1], Bryan P. Keary[1], Sophie Dixneuf[1,#], Robert Shalloo[2], Johannes Orphal[3]

[1]Department of Physics & Environmental Research Institute, University College Cork, Cork, Ireland
[2]Physics Department, University of Oxford, Denys Wilkinson Building, Keble Road, Oxford OX1 3RH, U.K.
[3]Karlsruhe Institute of Technology, Institute for Meteorology & Climate Research, D-76344 Eggenstein Leopoldshafen, Germany
[#]Currently with BIOASTER, Institut de recherche technologique, 321 avenue Jean Jaurès, 69007 Lyon, France

Introduction

Owing to its experimental simplicity, robustness, and (potential) cost efficiency, incoherent broadband cavity-enhanced absorption spectroscopy (IBBCEAS)[1] inspired a number of different experimental implementations in analytical and spectroscopic applications over the last 10 years. In IBBCEAS the transmission of broadband light through an optically stable cavity consisting of high reflectance mirrors (See Fig. 1.) is measured using incoherent sources of radiation e.g. xenon arc lamps, LEDs. The advantages of IBBCEAS include its high sensitivity, high temporal resolution, and large spectral coverage. However, one of the principle limitations to IBBCEAS is the coupling efficiency of incoherent light to high finesse optical cavities. This study [2] was motivated by the objective to find a way of increasing the amount of incoherent light inside a high finesse cavity without applying the principle of intra-cavity laser absorption spectroscopy (ICLAS)[3]. In contrast to ICLAS, this experiment was based on placing a "pulsed" high-temperature blackbody inside the cavity in the form of a laser-induced gas plasma, generated by a short pulse laser.

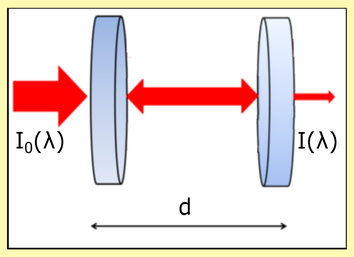

Fig. 1. Schematic of light passing an optical cavity. From the ratio of the wavelength-dependent transmitted intensities ($I_0(\lambda)$ and $I(\lambda)$), the effective reflectivity of the mirrors, $R_{eff}(\lambda)$ and the sample path length per pass, d, inside the cavity, the samples extinction coefficient, $\varepsilon(\lambda)$, can be calculated:

$$\varepsilon(\lambda) = \frac{1-R_{eff}(\lambda)}{d}\left(\frac{I_0(\lambda)}{I(\lambda)} - 1\right)$$

Experimental setup

A schematic of the experimental setup is shown in Fig. 2. The laser-induced breakdown in ambient lab air was generated with a Nd:glass laser, which, on its fundamental of 1055 nm, delivers pulses of ~2.6 mJ at a repetition rate of 27 Hz with a pulse duration of ca. 900 fs. Further compression of the pulse duration to ~200 fs was achieved with a KDP crystal.

In the present experiment, the fundamental and second harmonic at 527 nm were not separated, but both were focused with a fused-silica lens of 20 mm focal length to achieve a power density of ca. 1 TW/cm^2, assuming a beam waist of 25 µm and a 20% conversion efficiency. The laser-induced plasma was monitored as a function of wavelength and time using a monochromater (available gratings - 150, 600 or 1800 lines/mm, blaze at 500 nm) in conjunction with an iCCD camera.

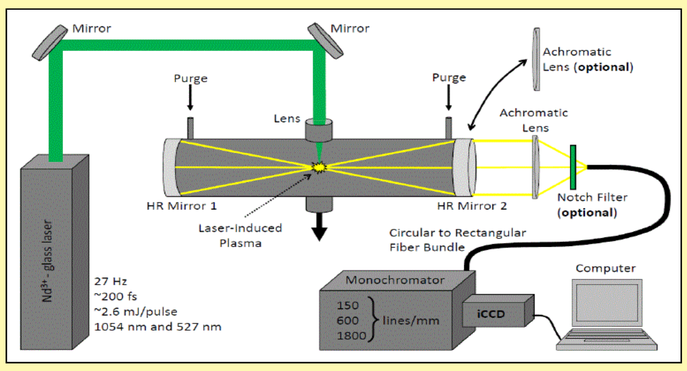

Fig. 2. Schematic of the experimental setup. The purge gas used in the cavity was either high grade N_2 or O_2. The volume between the HR mirrors was open to ambient lab air. In LIBS experiments without the cavity both HR mirrors were removed and HR mirror 2 was replaced by a second achromatic lens of an appropriate focal length.

Two different experimental configurations were used in this study:
(a) Direct plasma emission detection without a cavity.
(b) Generation of the plasma on the optical axis in the centre of a near-confocal cavity (Fig. 2) formed by two high-reflectivity mirrors.

Results of direct LIBS experiments

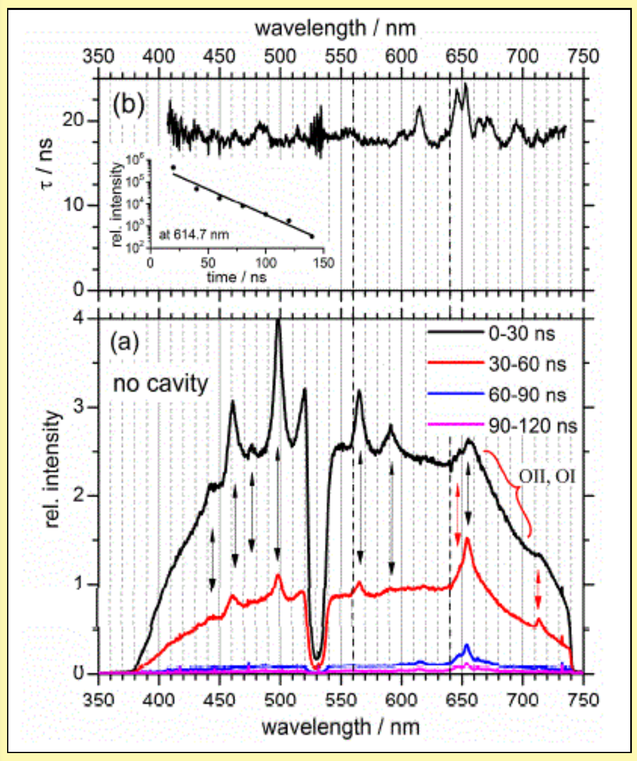

Fig. 3. (a) Relative intensity of the plasma emission as a function of wavelength for different times after the excitation. The dip at (530±8) nm is due to a notch filter. Black arrows correspond to emission features from NII, red ones to emissions from atomic OI.
(b) Characteristic exponential decay time, τ, as a function of wavelength. Insert: Typical mono-exponential fit referring to the intensity decay at 614.7 nm.

Fig. 3(a) shows the plasma emission spectra of ambient lab air at different times after laser excitation. The gated spectra were accumulated over 500 laser pulses and acquired in steps of 30 ns with a gate width of 30 ns. A grating with low dispersion (150 lines/mm, resolution ~2.8 nm) was used for the measurement.

Important in the context of this work is the time-dependence of the emission, because the direct LIBS experiments merely served as reference measurement to determine in-how-far the plasma emission can be sustained inside a cavity. A mono-exponential function empirically described the time-dependent intensity very well in the time range from the intensity maximum to ~140 ns. Fig. 3(b) shows the lifetime as a function of wavelength, based on contributions of the continuum emission lifetime due to plasma expansion and the decay times of excited species in the plasma. Generally the effective lifetimes vary between 15.6 and 31.3 ns, with a mean of (19.1±2.3) ns.

Results of plasma generation in high finesse cavity

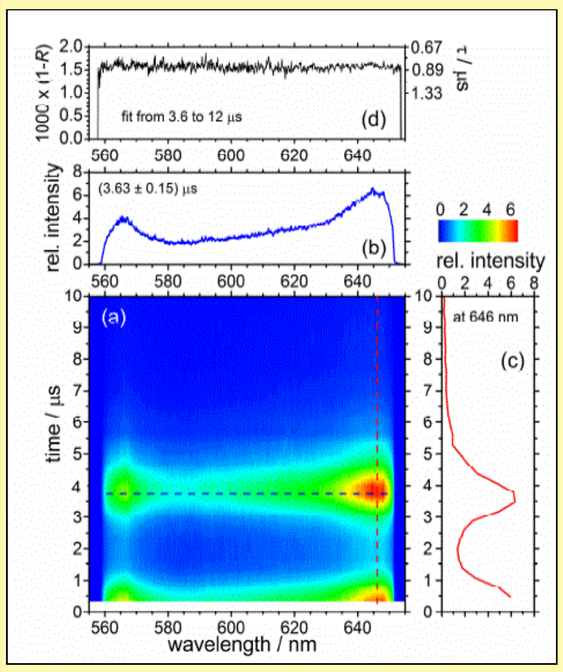

Fig. 4. (a) Measured intensity as a function of time and wavelength. (b) Spectrum in the second intensity maximum between 3.5 and 3.8 µs. (c) Emission time dependence at 646 nm. (d) Lifetime and corresponding value of (1 - R_{eff}) resulting from mono-exponential fit between 3.6 and 12 µs.

A laser-induced plasma was generated in ambient air at the centre of a quasi-confocal high finesse cavity and the relative emission intensity was measured outside the cavity. Fig. 4(a) illustrates this intensity as a function of time and wavelength.

It was determined that roughly 25 times less light was collected from the plasma with the cavity setup than with direct emission detection. As the light round trip time of the cavity is much shorter than the plasma lifetime, the absorption of the plasma during the initial phase of its temporal evolution plays a role in the significant lower photon signal. As seen in Fig. 4(c), the temporal evolution of the emission has a second maximum at 3.6 µs, the principle mechanism prolonging the emission without a gain process in the cavity is not yet understood.

One scenario that may explain the time dependence in Fig. 4(c) is based on the time dependent dimensions of the plasma in comparison to the beam waist in the cavity. Preliminary ray tracing calculations indicate that in the near-confocal cavity alignment, the size of the beam waist in the cavity varies periodically and therefore the light trapped in the cavity is periodically confined to length scales at the centre of the cavity that are comparable to the dimensions of the plasma, causing the time dependent losses.

Absorption spectra of gaseous azulene and O_2

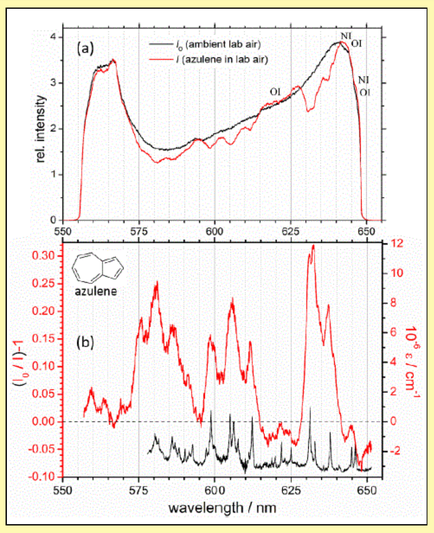

Fig. 5(a) shows the plasma emission of ambient air in the cavity, alongside that of azulene ($C_{10}H_6$). The wavelength-dependent optical loss due to azulene is visible in the spectrum. The resulting fractional absorption spectrum of gaseous azulene in air is shown in Fig. 5(b), where it is compared with the absorption spectrum from a previous study using a supersonic jet [4].

Fig. 5. (a) Light intensity leaking from the cavity in ambient air (black) and with azulene in ambient air (red). (b) Vibronic contour bands of the fractional $S_1 \leftarrow S_0$ absorption of azulene (red). Cavity ring-down absorption spectrum of azulene [4] shifted and scaled for comparison.

Fig. 6 shows the γ-absorption band of molecular oxygen:
$b^1\Sigma_g^+(v'=2) \leftarrow X^3\Sigma_g^-(v''=0)$. For this measurement the cavity was purged with a flow of oxygen at ca. 2 dm^3/min. The detected γ-band, with a band head at ~628 nm, is shown in Fig. 6 with a previously measured cavity ring-down spectrum for comparison [5]. A true I_0 signal (without molecular oxygen) was not measured in this case since the cavity was open to ambient air, thus Fig. 6 only shows the fractional absorption (red trace), whereby I_0 was simply taken as the linearly interpolated local background of the I(λ) spectrum.

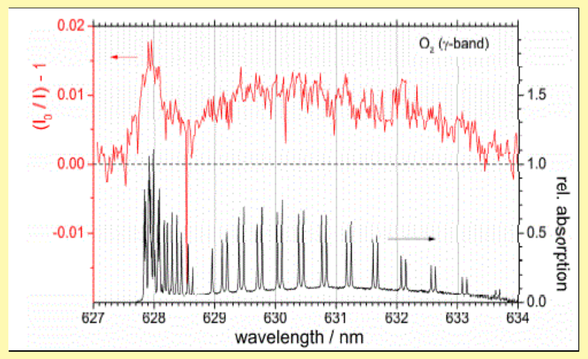

Fig. 6. Absorption spectra in molecular oxygen of the γ-band. Top: Fractional absorption measured by purging the cavity with oxygen into ambient air. Bottom: Cavity ring-down absorption spectrum for comparison. [5]

References

[1] S. E. Fiedler, A. Hese, and A. A. Ruth, Chem. Phys. Lett. 371, 284-294 (2003)
[2] A. A. Ruth, S. Dixneuf, and J. Orphal, Opt. Exp. 23(5), 6092-6101 (2015)
[3] V. M. Baev, T. Latz, and P. E. Toschek, Appl. Phys. B-Lasers Opt. 69, 171-202 (1999)
[4] A. A. Ruth, E. K. Kim, and A. Hese, Phys. Chem. Chem. Phys. 1, 5121-5128 (1999)
[5] A. A. Ruth, Physik. Blätter 55, 47-49 (1999)

Acknowledgments: The work was in parts funded through Science Foundation Ireland, Research Frontier Programme (contract: 11/RFP.1/PHY/3233), and through the INSPIRE Postdoctoral Programme (author SD) by the Irish Research Council for Science Engineering and Technology, co-funded through the Marie Curie Programme (COFUND) under framework FP7.